

# Multiple Regulatory Modules Are Required for Scale-to-Feather Conversion

Ping Wu,<sup>1</sup> Jie Yan,<sup>1,2</sup> Yung-Chih Lai,<sup>1,3,4</sup> Chen Siang Ng,<sup>5</sup> Ang Li,<sup>1</sup> Xueyuan Jiang,<sup>1</sup> Ruth M. Elsey,<sup>6</sup> Randall Widelitz,<sup>1</sup> Ruchi Bajpai,<sup>7</sup> Wen-Hsiung Li,<sup>8</sup> and Cheng-Ming Chuong<sup>\*,1,3,4,9,10</sup>

<sup>1</sup>Department of Pathology, Keck School of Medicine, University of Southern California, Los Angeles, CA

<sup>2</sup>Jiangsu Key Laboratory for Biodiversity and Biotechnology, College of Life Sciences, Nanjing Normal University, Nanjing, China

<sup>3</sup>Integrative Stem Cell Center, China Medical University Hospital, China Medical University, Taichung, Taiwan

<sup>4</sup>Research Center for Developmental Biology and Regenerative Medicine, National Taiwan University, Taipei, Taiwan

<sup>5</sup>Institute of Molecular and Cellular Biology & Department of Life Science, National Tsing Hua University, Hsinchu, Taiwan

<sup>6</sup>Louisiana Department of Wildlife and Fisheries, Rockefeller Wildlife Refuge, Grand Chenier, LA

<sup>7</sup>Center for Craniofacial Molecular Biology and Department of Biochemistry, University of Southern California, Los Angeles, CA

<sup>8</sup>Biodiversity Research Center, Academia Sinica, Taipei, Taiwan

<sup>9</sup>International Laboratory for Wound Repair and Regenerative Research, Graduated Institute of Clinical Medicine, National Cheng Kung University, Tainan, Taiwan

<sup>10</sup>Integrative and Evolutionary Galliformes Genomics Research Center (iEGG), National Chung-Hsing University, Taichung, Taiwan

\*Corresponding author: E-mail: cmchuong@med.usc.edu.

Associate editor: Gunter Wagner

The full data sets have been submitted to the NCBI Gene Expression Omnibus (GEO) under BioSample accession number GSE87250.

## Abstract

The origin of feathers is an important question in Evo-Devo studies, with the eventual evolution of vaned feathers which are aerodynamic, allowing feathered dinosaurs and early birds to fly and venture into new ecological niches. Studying how feathers and scales are developmentally specified provides insight into how a new organ may evolve. We identified *feather-associated genes* using genomic analyses. The candidate genes were tested by expressing them in chicken and alligator scale forming regions. Ectopic expression of these genes induced intermediate morphotypes between scales and feathers which revealed several major morphogenetic events along this path: Localized growth zone formation, follicle invagination, epithelial branching, feather keratin differentiation, and dermal papilla formation. In addition to molecules known to induce feathers on scales (retinoic acid,  $\beta$ -catenin), we identified novel scale-feather converters (*Sox2*, *Zic1*, *Grem1*, *Spry2*, *Sox18*) which induce one or more regulatory modules guiding these morphogenetic events. Some morphotypes resemble filamentous appendages found in feathered dinosaur fossils, whereas others exhibit characteristics of modern avian feathers. We propose these morpho-regulatory modules were used to diversify archosaur scales and to initiate feather evolution. The regulatory combination and hierarchical integration may have led to the formation of extant feather forms. Our study highlights the importance of integrating discoveries between developmental biology and paleontology.

**Key words:** Evo-Devo, stem cell, skin appendages, evolution, scale, bird, alligator, feather evolution, reprogramming.

## Introduction

Amniotes have various types of integumentary appendages including scales, feathers, and hair (fig. 1A; Wu, Hou et al. 2004). These appendages exhibit region-specific distributions on the body surface. For instance, many birds have scutate and reticulate scales on their lower legs and feet and have feathers on most of their remaining body parts. Crocodilians, such as American alligators, have different types of scales on their body surface (Alibardi and Thompson 2001). Some squamates, such as green iguanas, have elongated scales (Chang et al. 2009). The feather is a novel organ that evolved from dinosaur integuments. Developmental biology studies and recent fossil finds revealed that feathers evolved from a series of novel morphogenetic events (Prum 1999; Chuong

et al. 2000; Prum and Brush 2002; Wu, Hou et al. 2004; Xu et al. 2014; Brusatte et al. 2015).

The morphological evolution of feathers is a fundamental process of great interest because it produced a complex morphogenetic process with robust regeneration. Knowledge of this process is critical to understand how a new organ evolved that is used to define the Aves class of animals. The capacity of the avian shank dermis changes with advancing developmental stages (Rawles 1963). In epidermis/dermis recombination experiments, E9 shank dermis does not alter the fate of feather epidermis. However, at a later stage (E12) shank dermis can cause feather epidermis to form some scale-like skin appendages (Rawles 1963). Early studies explored the relationships between different skin appendages using hetero-class

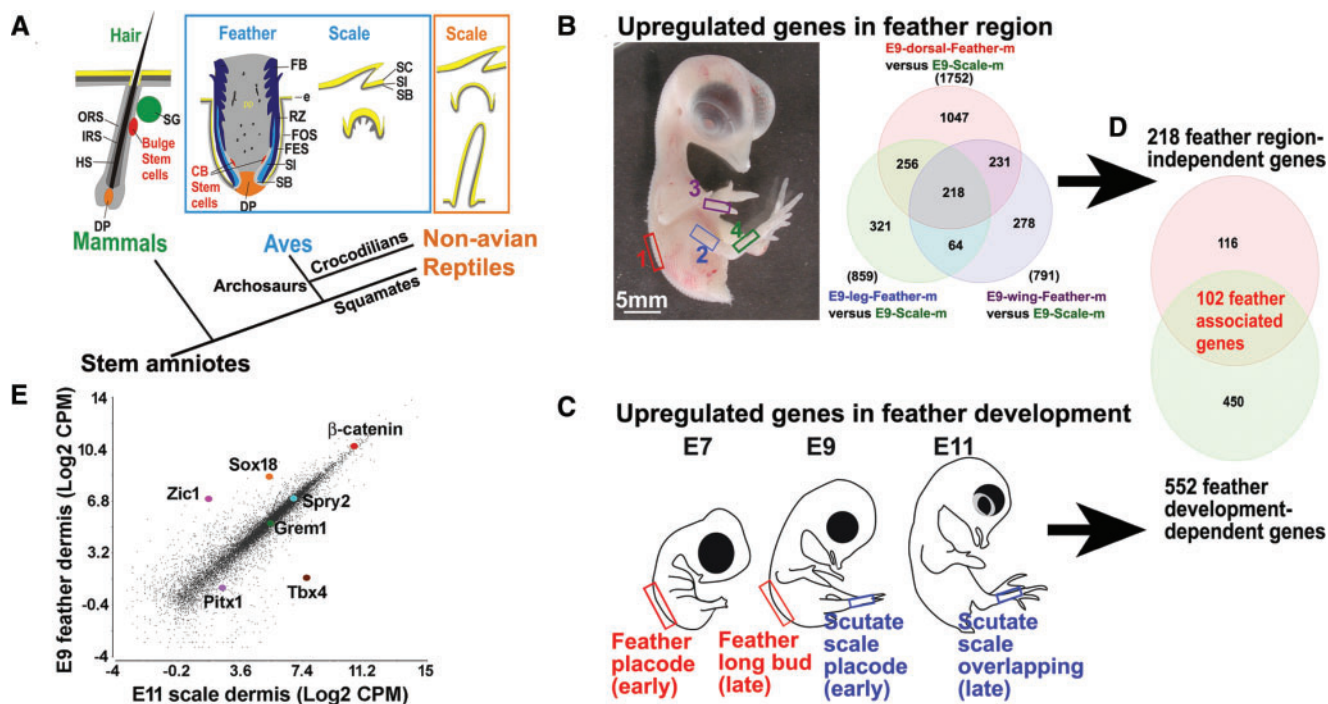


**FIG. 1.** Feather-associated genes revealed by RNA-seq. (A) Schematic drawing showing amniote skin appendages. Mammals have hairs. Chickens have feathers, scutate scales, and reticulate scales. The stem cell niche in hairs and feathers is marked in red. Other structures are also indicated. Alligators (crocodilians) have overlapping scales and tuberculate scales. Iguanas (squamates) have elongated scales. We focused on chicken scutate scales, alligator overlapping scales and iguana elongated scales in this paper. (B) 218 feather region-independent genes revealed by comparing transcriptome data from three different feather-forming regions (region 1-dorsal tract, 2-thigh tract, 3-wing tract) with the scutate scale-forming region (region 4). (C) 552 feather development-dependent genes revealed by comparing the transcriptome data for the feather region (placode stage-E7/bud stage-E9) with the scutate scale region (placode stage-E9 and bud stage-E11). (D) 102 feather-associated genes in common of B and C. (E) Scatter plot of feather and scale dermis at E9 and E11, respectively. *Pitx1* (purple) and *Tbx4* (brown) are the hind limb genes. Other dots are our candidate molecules. CB, collar bulge; DP, dermal papilla; e, epidermis; FB, feather barb ridge; FES, feather sheath; FOS, feather follicle sheath; HS, hair shaft; IRS, inner root sheath; ORS, outer root sheath; RZ, ramogenic zone; SG, sebaceous gland; SB, stratum basal; SC, stratum corneum; SI, stratum intermedium.

recombination. Exchanging the dermis of developing squamates and chicken skin showed scales can be induced by feather-forming dermis but the induced scales are arranged in feather patterns (Dhouailly 1975). Molecular studies revealed the involvement of several signaling pathways, such as the fibroblast growth factor (FGF), bone morphogenetic protein (BMP), and WNT pathways, in feather morphogenesis (Chen et al. 2015). Molecular perturbation with retinoic acid (RA; Dhouailly et al. 1980), Wnt/ $\beta$ -catenin (Widelitz et al. 2000), Notch/Delta pathway activation (Crowe and Niswander 1998), or BMP pathway suppression (Zou and Niswander 1996) can convert scales to feathers; we call these “scale-feather converters.” Comparative genomic studies identified conserved nonexonic elements that suggest exceptional regulatory innovation on the archosaur lineage. Also, the presence of feather development genes predates the appearance of feathers, signifying that the avian dinosaur ancestor already had the nonkeratin molecular toolkit necessary to make feathers (Lowe et al. 2015). However, how regulatory networks that specify feather morphology were established remains to be worked out. Genetic studies showed the feathered feet in pigeons and chickens are related to the cis-regulation of the limb determining genes *Pitx1* and *Tbx5* (Domyan et al. 2016). This conversion appears to involve

limb identity alterations (Logan and Tabin 1999; Rodriguez-Esteban et al. 1999; Takeuchi et al. 1999). How dermal tissues specify various integumentary appendage types (feather versus scale) remains unsolved.

Skin appendage fate determination (feathers vs. scales) is guided by epidermal–dermal interactions (Rawles 1963; Dhouailly 1975, 2009; Prin and Dhouailly 2004; Hughes et al. 2011). For instance, plantar epidermis is prevented to form feathers because of *En-1* expression (Prin and Dhouailly 2004). Here, we used transcriptome analyses and functional genomics to identify novel molecular circuits involved in scale-feather conversion. We identified five novel scale-feather converters, including three transcription factors (TFs), and two growth factor antagonists, which generate intermediate phenotypes. Intriguingly, some of these phenotypes are similar to the filamentous appendages found in the fossils of feathered dinosaurs (Xu et al. 2010; Persons and Currie 2015). We now have a potential molecular explanation for these hypothesized “missing links.” Our analyses led to identification of five morpho-regulatory modules that are essential for modern feather formation. We propose that the evolution of feathers required the integrative combination of five morpho-regulatory modules. The work here provides molecular clues of these modules.



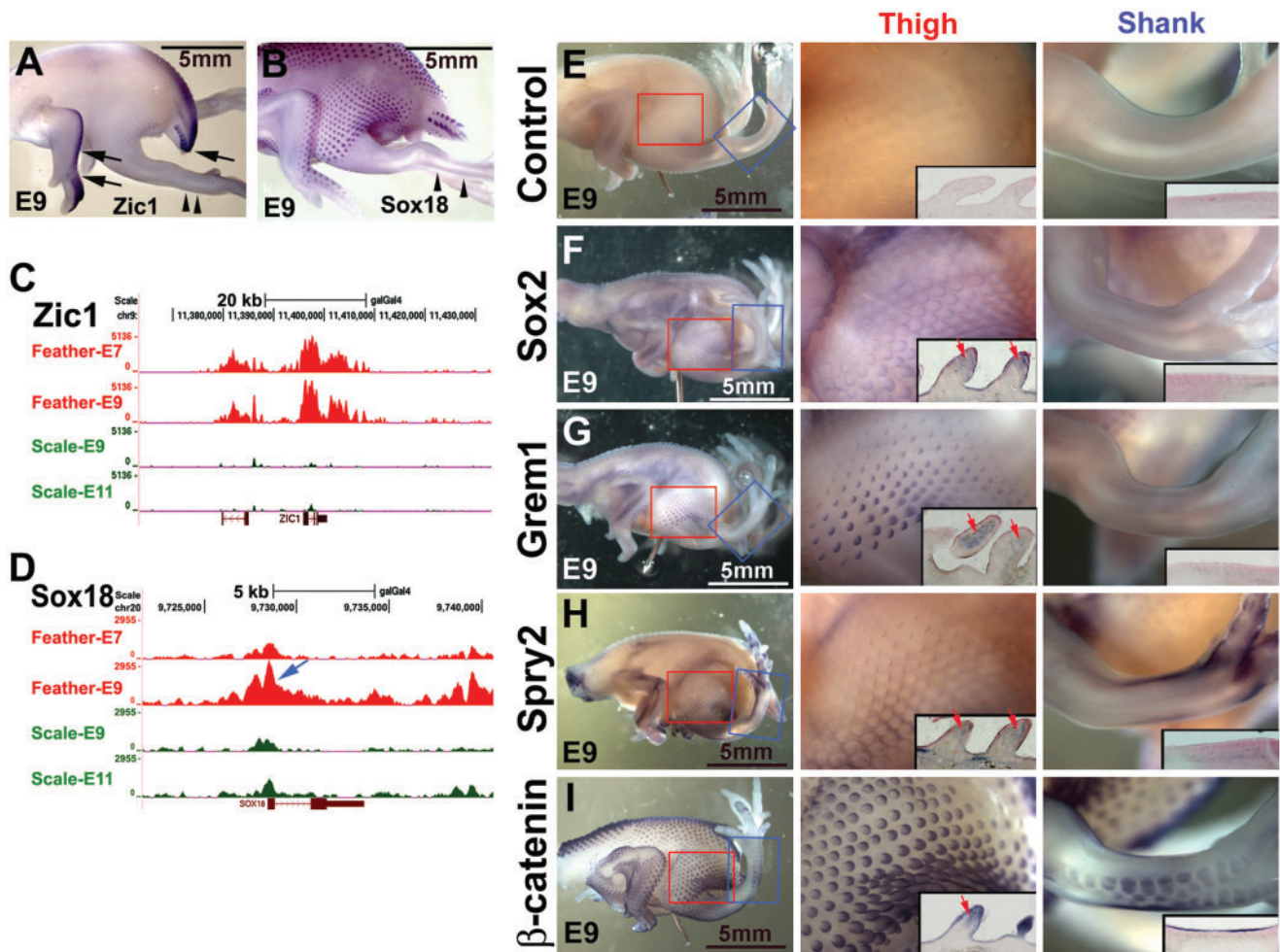


**FIG. 2.** Whole mount in situ hybridization and ChIP-seq analysis of chicken embryo candidate molecules. (A, B) WISH of E9 samples. (A) *Zic1*, Black arrows indicate higher *Zic1* expression levels in large feathers. (B) *Sox18*. Arrow heads indicate the lower expression in scale region. (C, D) Feather enhancers revealed by analyzing H3K27ac ChIP-seq data. Example of putative enhancers marked *Zic1* (C) and *Sox18* (D) gene. *Sox18* has strong H3K27ac mark (blue arrow) at late feather development stage (E9). Color in red and green are feather and scutate scale samples, respectively. (E) In situ hybridization control which lacks a specific probe. (F) *Sox2*. (G) *Grem1*. (H) *Spry2*. (I)  $\beta$ -*Catenin*. Columns 2 and 3 show higher magnification views of the thigh region (with feather buds) and shank region (with scutate scale placodes), respectively. Red arrows indicate expression in feather bud mesenchyme.

## Results

### Identification of Feather-Associated Genes

To understand the differential gene expression that may establish regional differences in skin appendage formation, we undertook multi-regional transcriptome analyses. We compared the mesenchyme from three E9 (H&H 35) feather-forming regions (wing, dorsal, and thigh) with the E9 scutate scale-forming region (fig. 1B). Hierarchical clustering and principle component analyses are shown in supplementary figure S1, Supplementary Material online. We found a trend of up-regulated gene expression in different tracts (enriched in dorsal feathers vs. scutate scales, 1,752 genes; thigh feathers vs. scutate scales, 859 genes; wing feathers vs. scutate scales, 791 genes). Together they shared 218 common up-regulated genes (fig. 1B, supplementary fig. S2A, Supplementary Material online), which we named *feather region-independent genes*. Next, we compared transcriptome data from body feathers and scutate

scales at two developmental stages, plastic (feather E7 [H&H 31], scutate scale E9) and determined stage (feather E9, scutate scale E11 [H&H 37]) (fig. 1C; Hughes et al. 2011). 552 up-regulated genes were found during embryonic feather development (fig. 1C, supplementary fig. S2C, Supplementary Material online), which we named *feather development-dependent genes*. We further named the intersection of the above two groups as *feather-associated genes* (fig. 1D, supplementary fig. S2E, Supplementary Material online). Of the 102 *feather-associated genes*, 12 encode TFs. Using the same strategy, we found 180 *scale-associated genes* (supplementary fig. S2B, D, F, Supplementary Material online).

We tested the function of *feather-associated genes* by focusing on the 12 TFs. Among them, *Zic1* and *Sox18* show high expression levels in feather-forming regions, but not in scutate scale-forming regions (fig. 1E). Whole mount in situ hybridization (WISH) confirms that these two TFs are expressed at lower levels in scale forming regions (fig. 2A and B,

arrowheads). *Zic1* also has enriched expression in the primordia of large feathers (fig. 2A; flight and tail feathers, black arrows).

To further evaluate the roles of feather-associated gene regulation, we conducted ChIP-seq analysis using H3K27ac, which is associated with active enhancer regions (Kouwenhoven et al. 2015) on both feather's and scale's plastic and determined stages. We found putative active enhancers overlapping with the *Zic1* gene in both E7 and E9 feather samples (fig. 2C) and *Sox18* in later feather developmental stages (fig. 2D, blue arrow). Thus, we identified two candidate TFs that may be critical in the feather-scale fate morphogenesis.

### Different “Scale-Feather Converters” Induce Different Intermediate Phenotypes

Beside candidate TFs *Zic1* and *Sox18* identified here, the role of Gremlin1 (*Grem1*, a BMP pathway antagonist) and Sprouty2 (*Spry2*, a receptor tyrosine kinase pathway antagonist) were tested as possible drivers of scale-feather conversion identified by microarray analysis (Hughes et al. 2011). Furthermore, we tested the expression and function of *Sox2* which is an embryonic multipotent stem cell marker and also is involved in mouse hair follicle development (Lesko et al. 2013). We propose that *Sox2* is potentially involved in early stage skin development. For comparison, we used molecules ( $\beta$ -catenin, RA) known to regulate scale to feather conversion as positive controls.

We performed WISH to observe the expression of these candidate molecules (*Sox2*, *Grem1*, and *Spry2*) in the developing feather and scutate scales (fig. 2E–I). WISH without a probe was used as a negative control (fig. 2E). WISH of  $\beta$ -catenin was used as a positive control (fig. 2I). We found that *Sox2*, *Grem1*, and *Spry2* were expressed in the mesenchyme of E9 thigh feather buds, but are negative in the dermis of shank scale placodes (fig. 2F, G, and H, red arrows). The expression of *Spry2* also was observed in the deep dermis of the shank (fig. 2H, right panel).  $\beta$ -Catenin was also expressed in the epidermis and mesenchyme of E9 feather buds (fig. 2I, red arrow).

We then carried out a series of functional studies of these nonbiased and biased candidates. We found a range of phenotypes (fig. 3A–F). The RCAS-GFP control did not alter the scutate scale shape (fig. 3A, A'). *Sox2* changed the scale-forming region to form periodically arranged bud like appendages on an otherwise flat skin (fig. 3B, B'). Overexpressing a constitutively active form of *Zic1* (*Zic1*- $\Delta$ C) caused scutate scales to display an irregular surface pattern suggesting invagination (fig. 3C, C', green arrow). *Grem1* induced a ridged scale surface that lacks follicle formation (fig. 3D, D'). *Spry2* converted scale-forming regions to exclusively feather-forming domains retaining the scale distribution pattern (fig. 3E, E'). Overexpression of *Sox18* in the scale-forming region induced a feather filament to form the distal edge of each scutate scale (fig. 3F, F', purple arrows), similar to that seen after ectopic  $\beta$ -catenin expression and RA treatment (Dhouailly et al. 1980; Widolitz et al. 2000).

We further characterize the phenotypes using *Shh* to monitor formation of placodes and barb ridges (fig. 3G–L), H&E

staining for the structure (fig. 4, first column), AMV-3C2 immunostaining for RCAS virus infection (fig. 4, second column), tenascin-C immunostaining for invagination and dermal papilla formation (fig. 4, third column), and  $\beta$ -keratin section in situ hybridization (SISH) for barb branch differentiation (fig. 4, fourth to seventh columns).

RA treatment induced *Shh* in early feather placodes that appeared from scales (Prin and Dhouailly 2004). We used *Shh* to track whether these molecular and chemical perturbations induced this early feather placode marker. WISH of *Shh* at E12 shows treated samples display different levels of feather-bud-like structures in the scutate scale region (fig. 3H–L), compared with controls in figure 3G. The *Sox2* overexpressing sample shows positive *Shh* expression in the ectopic buds (fig. 3H). The sample expressing *Zic1* shows decreased *Shh* levels in the scutate scales (fig. 3I). The bud induced by *Grem1* shows elongated scales with striped *Shh* expression (fig. 3J, enlarged in the inset, red lines). *Spry2* samples show ectopic *Shh* expression in feather-like-buds but lack the normal scutate scale *Shh* expression pattern (fig. 3K). The *Sox18* sample shows strong *Shh* expression in the induced feather-like-buds along with the regular *Shh* expression pattern in scutate scales (fig. 3L). These results show that different perturbations cause different levels of scale to feather conversion (fig. 3M), implying that shank skin has the capability to form feathers given the proper molecular signals.

H&E staining of E16 sections which represent a more mature stage further demonstrates the divergent skin appendage phenotypes induced in scale forming regions (fig. 4B–H, first column), compared with RCAS-GFP controls (fig. 4A, A', first column). Bud-like structures are observed in the *Sox2* sample (fig. 4B, first column). Longitudinal sections of *Zic1* samples indicate that an extra invagination lies beside the hinge region (fig. 4C, first column, black arrow). Cross sections show a clearer ridged structure in the scutate scale after *Grem1* overexpression (fig. 4D', compared with the longitudinal section in 4D). *Spry2* induced ectopic feathers are branched but lack follicular invaginations (fig. 4E, first column). Longitudinal sections of *Sox18*,  $\beta$ -catenin, and RA treated samples show that feather follicles forms on seemingly normal scutate scales (fig. 4F–H, first column).

To determine the location of RCAS virus infections, we performed AMV-3C2 immunostaining. We found that all RCAS transduced samples show epidermal and dermal AMV-3C2 staining (fig. 4, second column). A RA treated sample was used as a negative control for this immunostaining (fig. 4H, second column).

We further conducted tenascin-C immunostaining to investigate possible dermal papilla formation in the induced feather filament (fig. 4, third column). In normal E16 scutate scale, tenascin-C expressed in the outer surface dermis (fig. 4A, third column). In the normal feather, tenascin-C staining strongly expressed in the dermal papilla (fig. 4I, third column, red arrow; Jiang and Chuong 1992). Among the different molecular and chemical perturbed samples, only RCAS-*Sox18*, RCAS- $\beta$ -catenin, and RA treatment show faint tenascin-C staining in the region corresponding to the dermal papilla (fig. 4F–H, third column, green arrow heads).



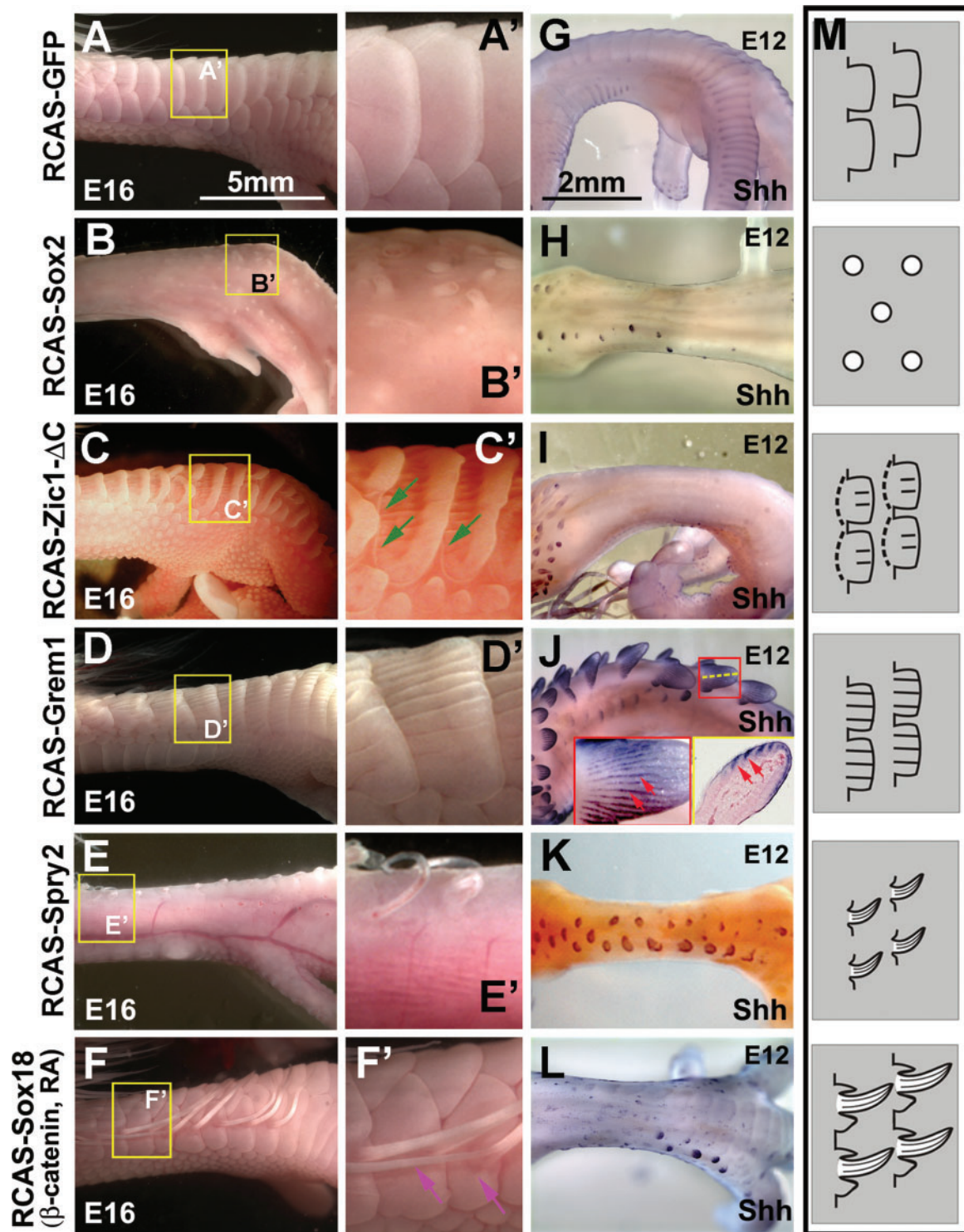


**Fig. 3.** Different perturbation phenotypes imply intermediate conversions from scutate scales to feathers. (A–F) Various phenotypes in the E16 scutate scale-forming region by different molecular perturbations. (A) RCAS-GFP control. (B) RCAS-Sox2. (C) RCAS-Zic1- $\Delta$ C. Green arrows indicate the invagination of scales. (D) RCAS-Grem1. (E) RCAS-Spry2. (F) RCAS-Sox18. Purple arrows indicate the feather filaments. (A'–F') High power view. (G–L) WISH of *Shh* in the perturbed samples at E12. Note the different types of feather-bud-like structures forming in the scutate scale region in panels J–L, compared with control in panel G. In panel J, the inset with a red frame is the enlarged bud and the inset with the yellow frame is a longitudinal section through the plane indicated by the yellow dotted line. These insets show barb ridge formation. Red arrows indicate *Shh* expression in the barb ridges. (M) Summary of different phenotypes induced by molecular and chemical perturbations.

This result indicates that *Sox18*,  $\beta$ -catenin, and RA induced feather-like structures which show some dermal papilla properties. The extra invagination in *Zic1* samples does not show

any tenascin-C staining (fig. 4C, third column) suggesting that while *Zic1* may initiate invagination step to form follicle, but it is not sufficient to form mature follicles.



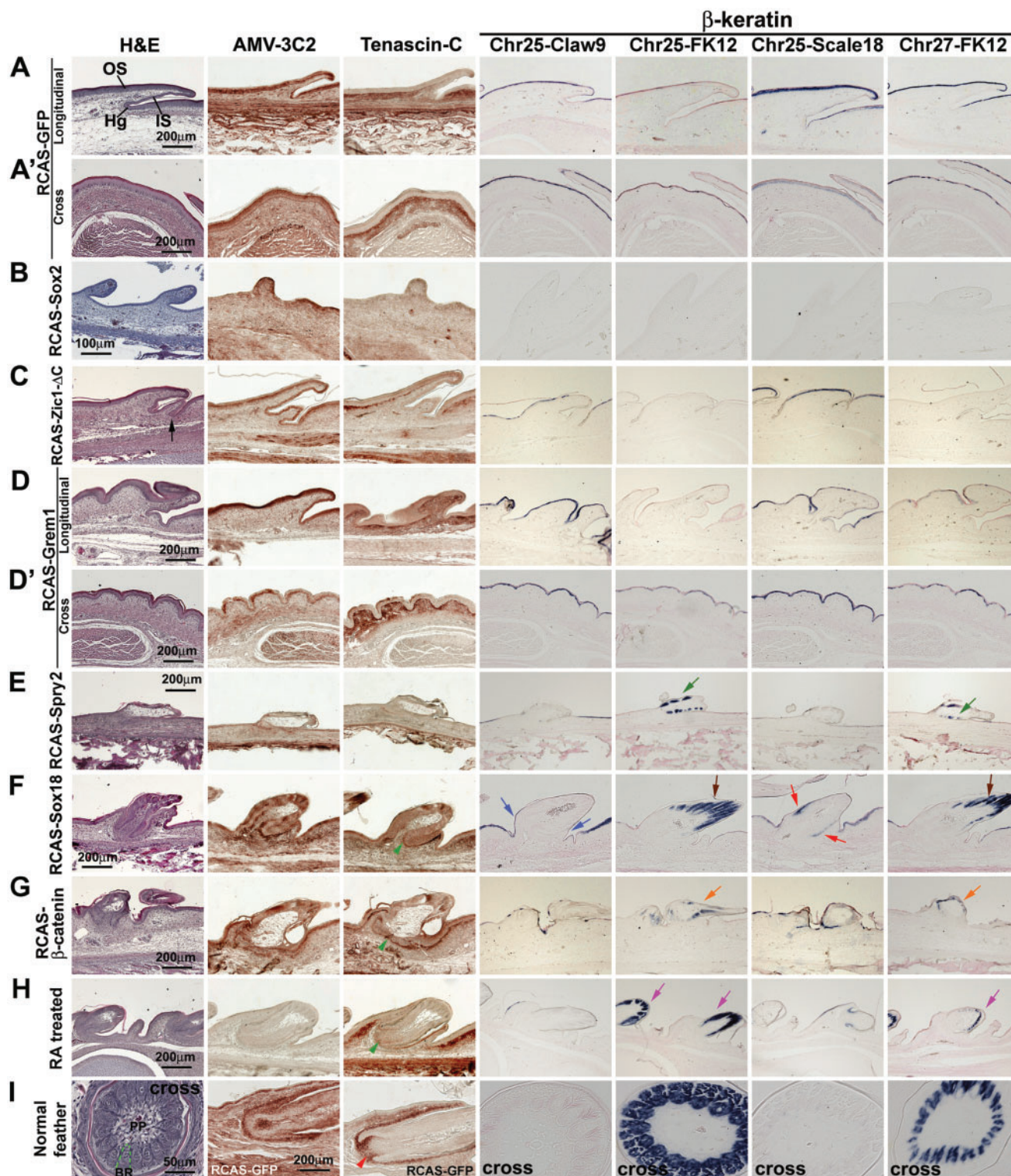


**FIG. 4.** Expression of AMV-3C2, tenascin-C and  $\beta$ -keratin genes after molecular and chemical perturbations at E16 chicken embryos. Column 1, H&E staining. Column 2, AMV-3C2 immunostaining. Column 3, tenascin-C immunostaining. Column 4–7, SISH of Chr25-Claw9, Chr25-FK12, Chr27-Scale18, and Chr27-FK12, respectively. (A–H) Longitudinal sections of the E16 scutate scale-forming region. (A' and D') Cross section. (A, A') RCAS-GFP scutate scale control. (B) RCAS-Sox2. (C) RCAS-Zic1- $\Delta$ C. Black arrow indicates the extra invagination. (D, D') RCAS-Grem1. (E) RCAS-Spry2. Green arrows indicate the scattered expression of feather  $\beta$ -keratins of both Chr25 and Chr27. (F) RCAS-Sox18. Blue arrows indicated the reduced Chr25-Claw9 expression. Brown arrows indicate the Chr25-FK12 and Chr27-FK12 in the barb ridges of induced feathers. Red arrows indicate the low level expression of Chr25-Scale18 in the lower feather sheath in the induced feather. (G) RCAS- $\beta$ -catenin. Orange arrow indicates the faint Chr25-FK12 and Chr27-FK12 gene expression. (H) RA treated. Purple arrows indicate the strong Chr25-FK12 and Chr27-FK12 expression in the induced feather filament. (I) Normal E16 feather (cross section) and RCAS-GFP infected E16 feather (longitudinal section). Dotted green line

### Uncoupling of Feather Morphogenesis from Feather $\beta$ -Keratin Differentiation

To determine whether the induced feather-like structures are real feathers with feather-specific keratinization, we did SISH using probes to four representative  $\beta$ -keratin genes with different appendage expression specificities (Chr25-claw9, Chr25-FK12, Chr25-Scale18, and Chr27-FK12). In normal E16 scutate scales, these four  $\beta$ -keratin genes are expressed on the scale epidermis, but with different patterns (Chr25-Claw9 keratin, periderm, and subperiderm; Chr25-FK12 and Chr27-FK12, periderm; Chr25-Scale18, subperiderm and stratum intermedium; Wu et al. 2015; fig. 4A, A', column 4–7). In embryonic feather development, feather keratins (FK) encoded on chromosomes 25 and 27 are differentially expressed in feather filament branches (Wu et al. 2015). In E16 feathers, both Chr25-FK12 and Chr27-FK12 are expressed in the barb ridge, but Chr27-FK12 is restricted to the barb cortex (Wu et al. 2015; fig. 4I, fifth column versus seventh column).

SISH revealed *Sox2* overexpressing samples lack expression of all four  $\beta$ -keratin genes (fig. 4B, column 4–7) which implies that *Sox2* treated samples are developmentally retarded, even if they have bud-like structures growing in the scale forming region. The *Zic1* overexpressing sample showed typical scale-like Chr25-Claw9 and Chr27-Scale18 expression patterns, but lack FK expression, even if phenotypically it shows invagination during scale development (fig. 4C, column 4–7). The mature *Grem1* overexpressing scales did not have strong FK expression (fig. 4D, D', column 4–7). This finding suggests these epithelial ridges on the surface of the scales do not represent normal barb ridges.

Feather  $\beta$ -keratin expression appears in the branches of the *Spry2* (fig. 4E, green arrows), *Sox18* (fig. 4F, brown arrows),  $\beta$ -catenin (fig. 4G, orange arrows), and RA treated samples (fig. 4H, purple arrows). *Spry2* samples express feather  $\beta$ -keratins from both Chr25 and Chr27, even though they lack the invagination phenotype (fig. 4E). *Sox18* overexpressing samples showed a feather specific  $\beta$ -keratin gene expression profile. The induced feather filament had reduced Chr25-Claw9 expression (blue arrows), enhanced Chr25-FK12 and Chr27-FK12 expression (brown arrows) and restricted Chr25-Scale18 expression in the base of the feather sheath (red arrows; fig. 4F). The  $\beta$ -keratin gene expression patterns in *Sox18* overexpressing samples are similar to that found in  $\beta$ -catenin overexpressing and RA treated samples (fig. 4G, H). These observations suggest that feather morphology and keratinization can be uncoupled during feather development. It is interesting to note that in hair follicle development, morphogenesis can be uncoupled from hair specific keratinization (Chiang et al., 1999).

We further analyzed the differential expression of  $\alpha$ - and  $\beta$ -keratin genes in the conversion of scales to feathers. By

comparing the RNA-seq data from the E16 samples, a list of the up- and down-regulated  $\alpha$ -keratin genes is presented in supplementary table S1, Supplementary Material online and  $\beta$ -keratin genes in supplementary table S2, Supplementary Material online. Notably, we found that claw and scale keratin genes on Chr25 are down-regulated in all treated samples, especially in the *Sox18*, RA, and *Sox2* samples, whereas feather-keratin genes on Chr25 are up-regulated the most in *Sox18* (11 out of 13) overexpressing and RA (9 out of 13) treated samples. In addition, the number of upregulated FK genes on Chr27 also is increased dramatically in *Sox18* (23 out of 63) and RA (38 out of 63) samples (supplementary table S2, Supplementary Material online). In contrast,  $\alpha$ -keratin gene expression profiling did not show any clear trend of altered expression in these treatments (supplementary table S1, Supplementary Material online). These different  $\beta$ -keratin expression profiles may reflect intermediate stages in the scale to feather transition.

### Avian Scale to Feather Conversion Requires Rebuilding of a Localized Growth Zone (LoGZ)

Next, we examined whether altering signaling molecule expression influences LoGZ formation during the scale to feather transition, using *Spry2* overexpression as an example (fig. 5A–F). *Spry2* induced feather bud formation in the scutate scale forming region (fig. 5B, compared with 5A). *Shh* WISH shows a higher expression level at the distal end of scale primordia (blue arrows in fig. 5D, compared with 5C). In addition, a focal cell proliferation pattern is coincident with the enhanced *Shh* expressing regions (fig. 5F). At the normal scutate scale developmental stage E10.5, cell proliferation still occurs in the interbud (fig. 5E). After *Spry2* misexpression, proliferation not only is restricted to the interbud at E10.5 but also becomes focal in the posterior bud region (fig. 5F, black arrows). These results suggest that proper feather induction from a scale primordium requires focal morphogen expression and the rebuilding of a LoGZ.

### Can One Induce Localized New Growth in Reptilian Scales?

Hair and feathers exhibit robust regenerative abilities following molting or plucking (Fuchs and Nowak 2008; Chuong et al. 2012). Alligator teeth can also undergo cyclic regeneration (Wu et al. 2013). So, can reptilian scales also undergo regeneration (fig. 6A–F)? Frills are elongated scales with a follicle-like structure (fig. 6B, D, and F). Wounded iguana frills (fig. 6G) did not activate new growth through a three month period, and then had only produced a new epidermal covering of the wound (fig. 6H). While invaginations surround the frills, there were no dermal papilla-like structures. Thus, the frill has very limited regeneration ability.

More intriguingly, we wondered whether one can induce a LoGZ on the reptilian scale to produce a new outgrowth.

FIG. 4. Continued

indicates a barb ridge. Red arrow head in panel (I) indicates tenascin-C staining in the feather dermal papilla. RCAS-*Sox18* (panel F), RCAS- $\beta$ -catenin (panel G) and RA treated samples (panel H) show faint tenascin-C staining in the region corresponding to the dermal papilla (green arrow heads). BR, barb ridge; Hg, hinge; IS, inner surface; OS, outer surface; PP, pulp.



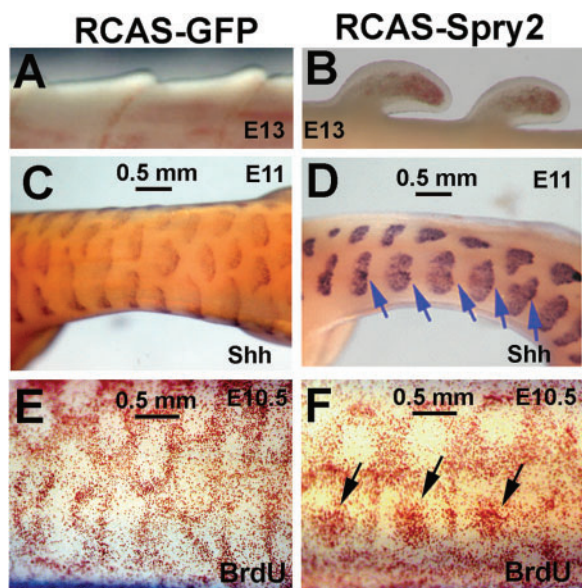


**Fig. 5.** *Spry2* induced focal *Shh* gene expression and LoGZ in scutate scale primordia. (A, C, E) RCAS-GFP control samples. (B, D, F) RCAS-*Spry2* samples. (A, B) Bright field view at E13. (C, D) *Shh* WISH at E11. Blue arrows in D indicate focal *Shh* gene expression in the distal end of scutate scale primordia. (E, F) Whole mount BrdU staining at E10.5. Black arrows in F indicate the LoGZs induced by *Spry2* overexpression.

To address this issue, we established an alligator skin explants culture system (fig. 6I) and did functional tests using two feather-scale converters (*Spry2* and  $\beta$ -catenin). Ectopically, expressing pEGFP-N1-*Spry2* in embryonic alligator skin demonstrated GFP expression after one day of culture (fig. 6J). After continuous culture for six days, we observed some outgrowth from the alligator skin (fig. 6K). These bud-like structures had extensive GFP expression, suggesting that the phenotype was induced by the ectopically expressed gene. Sections of these bud-like structures showed they resemble avian long feather buds (fig. 6L). However, no invagination or follicle formation was observed. These bud-like structures also had focal  $\beta$ -catenin expression (fig. 6M, orange arrow). Moreover, when we ectopically express  $\beta$ -catenin in the embryonic alligator skin we found elongated bud-like structures with invagination (fig. 6O, pink arrow), compared with control samples (fig. 6N). Our data suggest that these two scale-feather converters identified from birds can also induce ectopic LoGZ and grow feather bud-like elongated appendages from nonavian reptile skin.

## Discussion

The origin of avian scales is controversial. One view is that avian scales are homologues of nonavian reptile scales. However, it also has been hypothesized that bird scutate scales appeared later in evolution and are secondary structures derived from feathers (Dhouailly 2009). It is interesting that an ancient hatchling bird preserved in amber has both feathers and scales on their feet (Xing et al. 2017). Chicken scales changing to a feather morphology has been observed in domestic chickens (such as silkie) and in molecular biology experiments (Dhouailly et al. 1980; Tanaka et al. 1987;

Zou and Niswander 1996; Crowe and Niswander 1998; Wideltz et al. 2000). Even BrdU treatment can cause feather filament formation in the chicken shank (Tanaka et al. 1987). It seems that shank scales can be changed to feathers by the perturbation of several molecular pathways.

Here, we used a functional genomics approach to identify candidate genes for regional specificity determination. We manipulated several candidate molecules that convert scales into feathers by direct treatment with reagents or by virus-mediated overexpression. We were surprised to find that the phenotypes clustered into different morphotypes (fig. 3M), representing the activation of different morpho-regulatory modules and the expression of different feather specific keratins (supplementary table S2, Supplementary Material online). The five key feather morphogenetic events are: 1) a LoGZ that leads to elongated appendages, 2) invagination that leads to the formation of follicles, 3) barb ridge formation that leads to feather branching, 4) the expression of feather specific keratins, and 5) dermal papilla formation. Scales can be induced to elongate without folliculogenesis (*Sox2*, *Spry2*). Phenotypes produced in *Sox18*,  $\beta$ -catenin, and RA treated samples meet all of the five criteria necessary to be considered real feathers. The spectrum of these “intermediate morphotypes” suggests that the five key morphogenetic events can be un-coupled and specific criteria can be induced by specific molecular perturbations.

Some phenotypes generated by molecular perturbations are very intriguing. For example, *Sox2* changed the scale-forming region to form periodically arranged, *Shh* positive bud-like appendages on an otherwise flat skin (fig. 3B, B'). They do not mature to express FK like those induced by  $\beta$ -catenin or RA. Whether this perturbation of ectodermal fate can represent a reprogramming of cell fates, like what *Sox2* has been reported to do in other systems, remain to be studied with epigenetic tools in the future. Another interesting phenotype is from *Grem1*. We recently showed *Grem1* induced barb ridge formation in adult follicles (Li et al. 2017). In developing shank skin, *Grem1* caused different changes at different stages. In the earlier stages, *Grem1* caused parallel ridges with *Shh* positive stripes. They appear as periodically arranged *Shh* positive stripes (fig. 3J and insets). Since *Shh* is a marker for the marginal plate (Ting-Berretth and Chuong, 1996), we think these structures express morphological characteristics of barb ridges. However, the mature *Grem1* expressing scales show a ridged surface but lack proper feather specific keratin gene expression (fig. 4D, D'). This “novel” chimeric structure is evidence that morphogenesis and keratin differentiation can be uncoupled. How morphogenesis and keratin differentiation are coordinated properly at the genomic level to form barb ridges is a topic of great interest that remains to be investigated.

Some modern birds have filamentous integument appendages. Many birds have bristles, a simple feather type appearing on the face that consists of a rachis with either little or no branching. Bristles function like mammalian tactile whiskers (Persons and Currie 2015). Another example is the turkey beard, a specialized bristle with simple branches and FK expression but without a follicular structure (Sawyer et al. 2003).



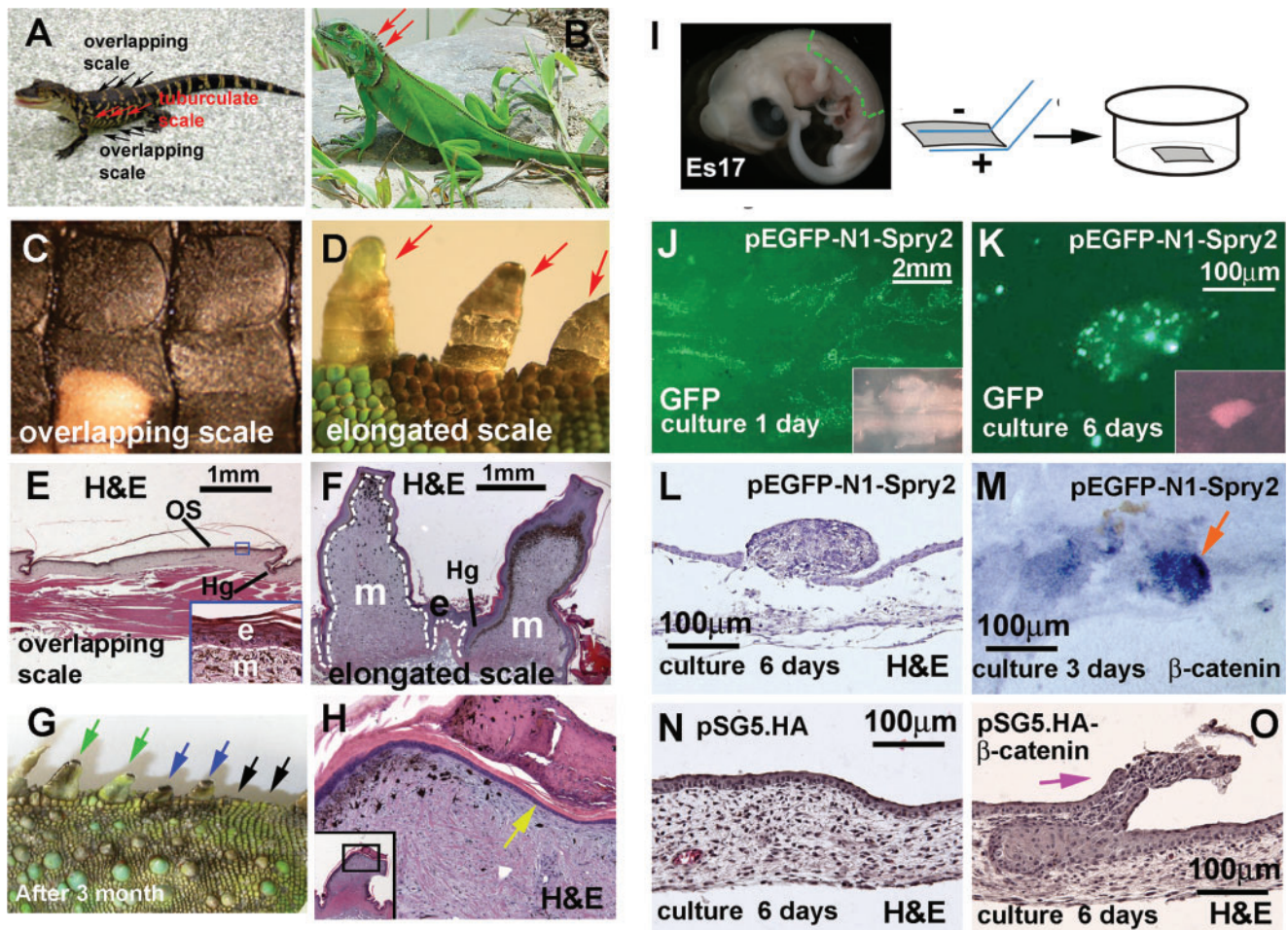


**FIG. 6.** Adult reptilian scales have limited endogenous regeneration ability but embryonic scales can be induced to grow a LoGZ. (A) Juvenile alligator with overlapping scales on dorsal and ventral side of the body. (B) Green iguana with elongated scales (frills) on the neck region. (C, D) Close view of alligator overlapping scales and iguana elongated scales. (E, F) H&E staining of scales. Inset in E showing the outer surface region. White dotted lines in E and F indicate the junction between epidermis and dermis. (G) Three months after part or whole elongated scales are surgically removed in the juvenile iguana. Green arrows, 1/3 of frills removed; blue arrows, 2/3 of frills removed; black arrows, all frills removed. (H) H&E staining of a wounded frill with newly formed epidermis covering the wound (yellow arrow). (I) Schematic drawing showing the culture system for embryonic alligator skin. The green dotted line indicates the dissected skin region for culture. (J–M) *Spry2* induced bud-like structures in alligator skin. (J) Expression of GFP in alligator dorsal skin (Es17) after electroporation with pEGFP-N1-*Spry2* (day 1). A bright field view of the same sample is shown in the inset. (K) Bud outgrowth (day 6), which is focally GFP positive. A bright field view is shown in the inset. (L) H&E staining of a section shows a bud-like structure. (M) WISH shows that *Spry2* induced bud-like structures (day 3) have strong  $\beta$ -catenin gene expression (orange arrow). (N, O), H&E staining of samples 6 days after electroporation with plasmid pSG5.HA (N) or pSG5.HA- $\beta$ -catenin (O). Pink arrow in O indicates the elongated bud-structure with invagination. e, epidermis; Hg, hinge; m, dermis; OS, outer surface.

Developing chicken scutate scales have slight dermal condensations until E13 (Sawyer 1972). Reptilian scales exhibit a placode configuration (Wu et al. 2014; Di-Poi and Milinkovitch 2016). Placodes can be traced back to fish scales (Harris et al. 2008). Both chicken feather and reptile scale placodes share the localization of nuclear  $\beta$ -catenin in early development (Musser et al. 2015). It is interesting that ectopic *Spry2* and  $\beta$ -catenin can induce new outgrowth not only from chicken scales but also from alligator scales.  $\beta$ -Catenin can even induce some invaginations and form elongated appendages, which share some characteristics similar to frills in iguanas. However, these morphologies are not sufficient to be called follicles. Intriguingly, we observed that frills fail to regenerate following injury. We speculate that this is

because they do not proceed to form a real follicle structure containing clustered stem cells and dermal papillae.

We summarize the spectrum of scale to feather conversion induced by molecular and chemical perturbations (fig. 7A). Different phenotypes may represent various combinations of the five feather defining criteria (fig. 7B). First, the formation of the appendage phenotype is determined by the interplay between the epithelium and mesenchyme. In this scenario, once committed to a certain fate, the dermis provides information of appendage identity to the epidermis. For appropriate skin appendage formation, the epidermis also needs to be in a competent state to receive the dermal signal and to respond accordingly. Classical tissue interaction experiments have been most inspiring. However, we now must try to discern the molecular basis for the response to these

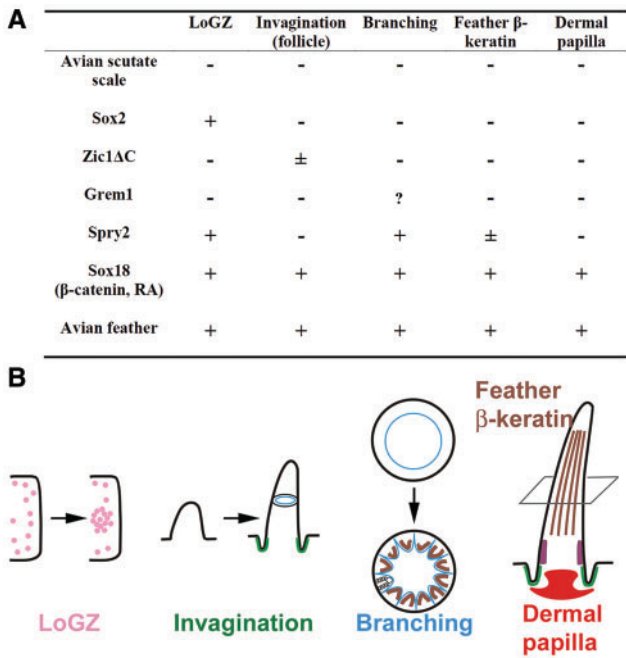


**FIG. 7.** Summary of intermediate phenotypes produced by molecular and chemical perturbations. (A) Intermediate phenotypes of scale to feather conversion as assessed by morphological alterations. – and + represent absence or presence of these feather characteristics. ? Represents ridged scales without mature barb ridge formation. *Shh* is used as a marker for placode (localized growth zone) and feather branching formation. *Tenascin-C* is used as the marker for follicle and dermal papilla formation. Feather  $\beta$ -keratin is used as the marker for feather differentiation. It is interesting to note that there is an uncoupling of morphogenesis (e.g. invagination, formation of early barb ridges) and differentiation (e.g. expression of feather  $\beta$ -keratin). (B) Schematic drawing shows the five properties of feathers including LoGZ, invagination, branching, feather  $\beta$ -keratin, and dermal papilla.

interactions, not only by assessing the morphogen experiments summarized in the introduction, but also by obtaining an understanding at the epigenetic level using current omics technologies. This study represents one major step toward this goal, but much work remains to be done.

Second, organ morphogenesis and histo-differentiation may be uncoupled. Some molecules only induce one of the five criteria. For example, *Sox2* can induce a LoGZ, but the feather buds do not mature into mature feather follicles. *Zic1* can induce an epithelial invagination process that mimics the initial step of follicle formation, but does not mature into a real feather follicle. *Grem1* can induce the branching morphogenetic process, but the *Grem1* transduced epithelium does not mature to form barb branches and does not express mature feather specific keratins. *Spry2* can co-activate several morpho-regulatory modules simultaneously, yet the scale forming region still does not form a complete feather follicle. Molecules, such as  $\beta$ -catenin, RA or *Sox18*, have a greater ability to form feather-like skin appendages with all criteria fulfilled.

Third, paleontological studies have revealed that nonavian dinosaurs had already acquired nonscale shaped skin appendages on their bodies. Branched scales were present in the

Triassic archosaur, *Longisquama* (Jones et al. 2000). Integuments with elongated cylindrical and filamentous structures existed broadly in different dinosaur lineages (Persons and Currie 2015). At least nine kinds of nonscale skin appendages have been found on the bodies of different dinosaur groups (Xu et al. 2010), ranging from simple filament-like to complex asymmetric flight feather-like structures. The strange, nonscale skin appendages found in non-avian dinosaurs suggest that successful feather evolution occurred in multiple steps, with different aspects of feather development evolving at different times and through the integration and coordination of distinct regulatory modules (table 1).

Our data suggest that a successful formation of feathers required the integration and coordination of these molecular modules. In this work, our developmental biology-based approach revealed molecules that are involved in each regulatory module. Our study provides ground work toward understanding how these regulatory modules are integrated at the molecular level for the generation of real feathers as defined by the five criteria.

### Materials and Methods

#### Chicken and Alligator Eggs

Pathogen-free fertilized chicken eggs were purchased from SPAFAS, Preston, CT. Chicken embryos were staged according to the method of Hamburger and Hamilton (1951). Alligator eggs collected from the Rockefeller Animal Refuge in Louisiana were incubated at 30 °C. Embryos staging was according to Ferguson (1985).

#### Whole WISH and SISH

Chicken embryos were collected, fixed in 4% paraformaldehyde at 4 °C overnight. For WISH, samples were dehydrated through a methanol series, embedded in paraffin and sectioned to 7  $\mu$ m. PCR primers for chicken *Sox18* are 5'-AATTAACCCTCACTAAAGGGAGAAGTATGGCTTGCCAACTCCC-3' (forward) and 5'-TAATACGACTCACTATA GGGAGAGGCGGATATCAAGCTGCTCT-3' (reverse). The PCR product was purified with a PCR Purification Kit (Qiagen) and then T7 polymerase (Roche) was used to make antisense the mRNA probe. PCR primers for chicken *Zic1* are 5'-CTACGTTCCGATCGTCTCG-3' (forward) and 5'-CATCTGCCCCGTTACCAC-3' (reverse). PCR primers for chicken *Sox2* are 5'-AGAACCCGAAGATGCACAAC-3' (forward) and 5'-CCTTGCTGGGAGTACGACAT-3' (reverse). The PCR product was inserted into the p-drive plasmid (Qiagen). cDNA from a stage 24 chicken embryo was used for the DNA template.

Chicken  $\beta$ -catenin and *Shh* probes were used according to Widelitz et al. (2000). Chicken *Grem1* probe is from (Capdevila et al. 1999). Chicken *Spry2* probe is from (Minowada et al. 1999). Chicken  $\beta$ -keratin probes are used according to Wu et al. (2015). Alligator  $\beta$ -catenin probe is described in Wu et al. (2013). Digoxigenin-labeled nucleotides were incorporated into RNA riboprobes transcribed in vitro from linearized cDNAs. In situ hybridization was performed as



**Table 1.** Different Skin Appendage Phenotypes in Stem Amniotes, Living Reptiles, and Extant Avian Species.

	LoGZ	Invagination (Follicle)	Branching	Feather $\beta$ -Keratin	Dermal Papilla
Reptilian overlapping scale	—	—	—	—	—
Reptilian frill	+	+	—	—	—
Dinosaur elongate cylindrical and filamentous integument (Persons and Currie 2015)	+	?	—	?	—
Feathered dinosaur (morphotype 1–2) (Xu et al. 2010)	+	?	—	?	—
Feathered dinosaur (morphotype 3–9) (Xu et al. 2010)	+	+	+	?	+
Turkey beards (Sawyer et al. 2003)	+	—	+	+	—
Avian feather	+	+	+	+	+

NOTE.— — and +represents absence or presence of these characteristics.? Represents unknown.

described (Ting-Berreth and Chuong 1996). After SISH, faint eosin staining was used for counter-staining.

Section Immunostaining

Section immunostaining and antibody to tenascin-C was performed as described (Chuong and Chen 1991). AMV-3C2 antibody is from the Developmental Studies Hybridoma Bank.

Whole Mount BrdU Staining

For BrdU staining of chicken embryos, 10  $\mu$ l 1% BrdU was injected to a vein. After 2 h the embryos were fixed in methanol and prepared for whole mount BrdU immunostaining following the procedure of Wu, Jiang et al. (2004).

RCAS Infection

For RCAS (replication-competent avian sarcoma virus) mediated gene misexpression, full length chicken Sox2 (PCR primers: 5'-GGGGACAAGTTTGTACAAAAAAGCAGGCTTCA CCATGTACAACATGATGGAAAC-3' [forward], 5'-GGGGA CCACTTTGTACAAGAAAGCTGGGTCTCACATATGTGA TAGAGGGA-3' [reverse]), full length chicken Sox18 (PCR primers: 5'-GGGGACAAGTTTGTACAAAAAAGCAGGC TTCACCATGAATATATCTGAGTCAAAC-3' [forward], 5'-GGGGACCACTTTGTACAAGAAAGCTGGGTCTAGCC GGTGATGCATGGGCT-3' [reverse]) and chicken Zic1- $\Delta$ C (a C-terminally truncated form with enhanced transcriptional activation activity) (PCR primers: 5'-GGGGAC AAGTTTGTACAAAAAAGCAGGCTTCACCATGCTTCTGG ATGCTGGACCGCA-3' [forward], 5'-GGGGACCACTTTGT ACAAGAAAGCTGGGTCTTAAGACACGATGGTTGGAG-3' [reverse]) (Kuo et al. 1998; Merzdorf and Sive 2006) were cloned into RCAS using the Gateway system (Loftus et al. 2001). RCAS-chicken-Grem1 (RCAS-Grem1), RCAS-Xenopus- $\beta$ -catenin armadillo fragment (RCAS- $\beta$ -catenin) and RCAS-mouse-Sprouty2 (RCAS-Spry2) plasmids was kindly provided by Dr Izpisua Belmonte (Capdevila et al. 1999), Dr Johnson (Capdevila et al. 1998), and Dr Minowada (Minowada et al. 1999), respectively.

RCAS retrovirus was prepared and titrated by transfecting chicken embryo fibroblasts following the protocol described (Jiang et al. 1998). Four microliter of concentrated RCAS viruses was injected to the amniotic cavity and hind limb at E3 (stage 18) chicken embryos. The alternative method is

injecting 4  $\mu$ l RCAS plasmid (1  $\mu$ g/ $\mu$ l) to the amniotic cavity and hind limb followed by electroporation. The electric current was delivered as 3 pulses of 15 V/50 ms. Infected samples were collected at E10–E16 (stage 36–42). Controls include an RCAS vector driving GFP expression. At least three replicates were collected for each condition at different time points.

RA Treatment

RA (all-trans RA, RA, Sigma) was dissolved in absolute ethanol and 30  $\mu$ g of RA was injected into the amniotic cavity at E9. Samples were collected at E10–E16 (stage 36–42).

Electroporation of Spry2 and  $\beta$ -Catenin to Alligator Embryonic Skin

E817-18 alligator embryonic dorsal skins were collected and electroporated with pEGFP-N1-*mSpry2* (a gift from Dr Warburton, Tefft et al. 2002) or pSG5.HA- $\beta$ -catenin (from Dr Stallcup, Koh et al. 2002) (1  $\mu$ g/ $\mu$ l). Electroporation was performed with the negative pole faces the epithelium. The electric current was delivered as 3 pulses of 15 V/50 ms. pEGFP-N1 and pSG5.HA were used as controls. Skin explants then were transferred to culture inserts in six-well culture dishes (Falcon) and cultured in DMEM media (Gibco/BRL) with 10% fetal calf serum (Gemini) containing 1 $\times$  Antibiotic Antimycotic solution (Sigma). The explants were incubated at 35  $^{\circ}$ C at an atmosphere of 5% CO<sub>2</sub> and 95% air up to 6 days.

Juvenile Green Iguana Scale Regeneration

The juvenile iguana was anesthetized. Six frills in three different experimental groups are excised. In group 1, 2 and 3, 1/3, 2/3 or whole frills above the skin were removed, respectively. Animals were euthanized after 3 months.

RNA-Seq Analysis

RNA-seq analysis on normal chicken skin development was performed on two sets of samples. 1) Replicate samples from four regions of E9 (H&H stage 35) chicken embryos. These regions include three feather-forming regions (dorsal, wing, and thigh) and the scutate scale-forming tarsometatarsal region. 2) Replicate samples from the dorsal tract feather-forming region (E7 [stage 31] and E9 [stage 35]), and leg scutate scale-forming region (E9 [stage 35] and E11 [stage 37]). Epidermis and dermis were separated by treating with

2XCMF solution. For RCAS virus infected and GFP control samples, we collected tarsometatarsal skin at E16 (stage 42). Both epidermis and dermis are used since we cannot separate the E16 feather's epidermis and dermis. RNA was extracted using Trizol reagent (Invitrogen). 0.5–1 µg of total RNA from each sample was used to construct an RNA-seq library using TruSeq RNA sample preparation v2 kit (Illumina). Sequencing (50 or 75 cycles single read) was performed using Hi-seq 2000 or NextSeq 500 at the USC Epigenome Center. All of the RNA-seq samples are listed in supplementary table S3, Supplementary Material online.

### Read Mapping and Transcriptome Analyses

TopHat2 was used for alignment. HTSeq-count was used for quantification. If the fragments were multiply mapped on different genes, the reads were removed from analysis. The weighted trimmed mean of the log expression ratios (trimmed mean of *M* values, TMM) were used for normalization (Robinson and Oshlack 2010). Genes differentially expressed among embryonic samples were determined by edgeR (Robinson and Smyth 2008). False discovery rate (FDR) < 0.05 was used as a threshold to determine significant differences in gene expression.

### Keratin Analysis

The keratin analysis uses the method of Wu et al. (2015). Briefly, RNA-seq data were aligned with annotated chicken keratin genes in Galgal4-72 (Ng et al. 2014). Differential expression was analyzed among different groups of samples with a FDR < 0.05. Hierarchical clustering analysis was performed with Partek Genomic Suite using the Squared Euclidean Distance and grouped according to Ward's method.

### ChIP-Seq

To perform ChIP-seq, embryonic skin was treated with 2 ml 0.35% collagenase (type I) at 37 °C for 30 min to 1 h. Chromatin prepared from different skin samples was immunoprecipitated with an H3K27ac antibody (abcam ab4729). IgG and input DNA were used as background controls. ChIP protocol was according to Boyer et al. (2005). Precipitated DNA was used to generate sequencing libraries using NEBNext Ultra DNA Library kit. All of the ChIP-seq samples are listed in supplementary table S3, Supplementary Material online. The enriched regions are analyzed using MACS peak calling software (Zhang et al. 2008). The replicates of each sample group are combined to perform peak calling. The enrichment profiles are visualized using the UCSC genome browser.

### Supplementary Material

Supplementary data are available at *Molecular Biology and Evolution* online.

### Acknowledgments

The authors thank Dr Roger Sawyer and Dr Travis Glenn for their help and discussions for this project. We also thank the USC Epigenome Core Facility for conducting next generation

sequencing. In addition, we also wish to thank Yibu Chen and Meng Li of the USC Norris library for help with bioinformatics analysis. Research reported in this publication was supported by the National Institute of Arthritis and Musculoskeletal and Skin Diseases of the National Institutes of Health, USA under Award Numbers AR 47364 and AR 60306 and by the Ministry of Science and Technology, Taiwan (MOST 104-2621-B-001-003-MY3; MOST-105-3111-Y-001-040). The content is solely the responsibility of the authors and does not necessarily represent the official views of the National Institutes of Health.

### Author Contributions

P.W., R.W., R.B., W.-H.L., and C.-M.C. designed the experiments. P.W., J.Y., A.L., R.E., and X.J. carried out the experiments. Y.-C.L. and C.S.N. carried out the bioinformatics analyses. P.W., R.W., W.-H.L., and C.-M.C. wrote the manuscript with input from all authors.

### References

- Alibardi L, Thompson MB. 2001. Scale morphogenesis and ultrastructure of dermis during embryonic development in the alligator. *Acta Zool.* 81(4):325–338.
- Boyer LA, Lee TI, Cole MF, Johnstone SE, Levine SS, Zucker JP, Guenther MG, Kumar RM, Murray HL, Jenner RG, et al. 2005. Core transcriptional regulatory circuitry in human embryonic stem cells. *Cell* 122(6):947–956.
- Brusatte SL, O'Connor JK, Jarvis ED. 2015. The origin and diversification of birds. *Curr Biol.* 25(19):R888–R898.
- Capdevila J, Tabin C, Johnson RL. 1998. Control of dorsoventral somite patterning by Wnt-1 and beta-catenin. *Dev Biol.* 193(2):182–194.
- Capdevila J, Tsukui T, Rodríguez Esteban C, Zappavigna V, Izpisua Belmonte JC. 1999. Control of vertebrate limb outgrowth by the proximal factor Meis2 and distal antagonism of BMPs by Gremlin. *Mol Cell.* 4(5):839–849.
- Chang C, Wu P, Baker RE, Maini PK, Alibardi L, Chuong CM. 2009. Reptile scale paradigm: Evo-Devo, pattern formation and regeneration. *Int J Dev Biol.* 53(5–6):813–826.
- Chen CF, Foley J, Tang PC, Li A, Jiang TX, Wu P, Widelitz RB, Chuong CM. 2015. Development, regeneration, and evolution of feathers. *Annu Rev Anim Biosci.* 3:169–195.
- Chiang C, Swan RZ, Grachtchouk M, Bolinger M, Litingtung Y, Robertson EK, Cooper MK, Gaffield W, Westphal H, Beachy PA, et al. 1999. Essential role for Sonic hedgehog during hair follicle morphogenesis. *Dev Biol.* 205(1):1–9.
- Chuong CM, Chen HM. 1991. Enhanced expression of neural cell adhesion molecules and tenascin (cytotactin) during wound healing. *Am J Pathol.* 138(2):427–440.
- Chuong CM, Chodankar R, Widelitz RB, Jiang TX. 2000. Evo-Devo of feathers and scales: building complex epithelial appendages. *Curr Opin Genet Dev.* 10(4):449–456.
- Chuong CM, Randall VA, Widelitz RB, Wu P, Jiang TX. 2012. Physiological regeneration of skin appendages and implications for regenerative medicine. *Physiology (Bethesda)* 27(2):61–72.
- Crowe R, Niswander L. 1998. Disruption of scale development by Delta-1 misexpression. *Dev Biol.* 195(1):70–74.
- Dhouailly D. 1975. Formation of cutaneous appendages in dermoepidermal recombinations between reptiles, birds and mammals. *Wilhelm Roux' Arch Entwicklungsmech Org.* 177(4):323–340.
- Dhouailly D. 2009. A new scenario for the evolutionary origin of hair, feather, and avian scales. *J Anat.* 214(4):587–606.
- Dhouailly D, Hardy MH, Sengel P. 1980. Formation of feathers on chick foot scales: a stage-dependent morphogenetic response to retinoic acid. *J Embryol Exp Morphol.* 58:63–78.



- Di-Poi N, Milinkovitch MC. 2016. The anatomical placode in reptile scale morphogenesis indicates shared ancestry among skin appendages in amniotes. *Sci Adv.* 2(6):e1600708.
- Domyan ET, Kronenberg Z, Infante CR, Vickrey AI, Stringham SA, Bruders R, Guernsey MW, Park S, Payne J, Beckstead RB, et al. 2016. Molecular shifts in limb identity underlie development of feathered feet in two domestic avian species. *Elife* 5:e12115.
- Ferguson MW. 1985. The reproductive biology and embryology of crocodilians. In: Gans C, Billet F, Maderson P, editors. *Biology of the reptilia*. New York: Wiley. p. 451–460.
- Fuchs E, Nowak JA. 2008. Building epithelial tissues from skin stem cells. *Cold Spring Harb Symp Quant Biol.* 73:333–350.
- Hamburger V, Hamilton HL. 1951. A series of normal stages in the development of the chick embryo. *J Morphol.* 88(1):49–92.
- Harris MP, Rohner N, Schwarz H, Perathoner S, Konstantinidis P, Nüsslein-Volhard C. 2008. Zebrafish *eda* and *edar* mutants reveal conserved and ancestral roles of ectodysplasin signaling in vertebrates. *PLoS Genet.* 4(10):e1000206.
- Hughes MW, Wu P, Jiang TX, Lin SJ, Dong CY, Li A, Hsieh FJ, Widelitz RB, Chuong CM. 2011. In search of the Golden Fleece: unraveling principles of morphogenesis by studying the integrative biology of skin appendages. *Integr Biol (Camb)* 3(4):388–407.
- Jiang T, Stott N, Widelitz R, Chuong C. 1998. Current methods in the Study of Avian Skin Appendages. In: Chuong C, editor. *Molecular basis of epithelial appendage morphogenesis*. Austin (TX): Landes Bioscience. p. 395–408.
- Jiang TX, Chuong CM. 1992. Mechanism of skin morphogenesis. I. Analyses with antibodies to adhesion molecules tenascin, N-CAM, and integrin. *Dev Biol.* 150(1):82–98.
- Jones TD, Ruben JA, Martin LD, Kurochkin EN, Feduccia A, Maderson PF, Hillenius WJ, Geist NR, Alifanov V. 2000. Nonavian feathers in a late Triassic archosaur. *Science* 288(5474):2202–2205.
- Koh SS, Li H, Lee YH, Widelitz RB, Chuong CM, Stallcup MR. 2002. Synergistic coactivator function by coactivator-associated arginine methyltransferase (CARM) 1 and beta-catenin with two different classes of DNA-binding transcriptional activators. *J Biol Chem.* 277(29):26031–26035.
- Kouwenhoven EN, Oti M, Niehues H, van Heeringen SJ, Schalkwijk J, Stunnenberg HG, van Bokhoven H, Zhou H. 2015. Transcription factor p63 bookmarks and regulates dynamic enhancers during epidermal differentiation. *EMBO Rep.* 16(7):863–878.
- Kuo JS, Patel M, Gamse J, Merzdorf C, Liu X, Apekin V, Sive H. 1998. Opl: a zinc finger protein that regulates neural determination and patterning in *Xenopus*. *Development* 125(15):2867–2882.
- Lesko MH, Driskell RR, Kretschmar K, Goldie SJ, Watt FM. 2013. Sox2 modulates the function of two distinct cell lineages in mouse skin. *Dev Biol.* 382(1):15–26.
- Li A, Figueroa S, Jiang TX, Wu P, Widelitz R, Nie Q, Chuong CM. 2017. Diverse feather shape evolution enabled by coupling anisotropic signalling modules with self-organizing branching programme. *Nat Commun.* 8:ncmms14139.
- Loftus SK, Larson DM, Watkins-Chow D, Church DM, Pavan WJ. 2001. Generation of RCAS vectors useful for functional genomic analyses. *DNA Res.* 8(5):221–226.
- Logan M, Tabin CJ. 1999. Role of Pitx1 upstream of Tbx4 in specification of hindlimb identity. *Science* 283(5408):1736–1739.
- Lowe CB, Clarke JA, Baker AJ, Haussler D, Edwards SV. 2015. Feather development genes and associated regulatory innovation predate the origin of Dinosauria. *Mol Biol Evol.* 32(1):23–28.
- Merzdorf CS, Sive HL. 2006. The *zic1* gene is an activator of Wnt signaling. *Int J Dev Biol.* 50(7):611–617.
- Minowada G, Jarvis LA, Chi CL, Neubüser A, Sun X, Hacohen N, Krasnow MA, Martin GR. 1999. Vertebrate *Sprouty* genes are induced by FGF signaling and can cause chondrodysplasia when overexpressed. *Development* 126(20):4465–4475.
- Musser JM, Wagner GP, Prum RO. 2015. Nuclear  $\beta$ -catenin localization supports homology of feathers, avian scutate scales, and alligator scales in early development. *Evol Dev.* 17(3):185–194.
- Ng CS, Wu P, Fan WL, Yan J, Chen CK, Lai YT, Wu SM, Mao CT, Chen JJ, Lu MY, et al. 2014. Genomic organization, transcriptomic analysis, and functional characterization of avian  $\alpha$ - and  $\beta$ -keratins in diverse feather forms. *Genome Biol Evol.* 6(9):2258–2273.
- Persons WS, Currie PJ. 2015. Bristles before down: a new perspective on the functional origin of feathers. *Evolution* 69(4):857–862.
- Prin F, Dhouailly D. 2004. How and when the regional competence of chick epidermis is established: feathers vs. scutate and reticulate scales, a problem en route to a solution. *Int J Dev Biol.* 48(2–3):137–148.
- Prum RO. 1999. Development and evolutionary origin of feathers. *J Exp Zool.* 285(4):291–306.
- Prum RO, Brush AH. 2002. The evolutionary origin and diversification of feathers. *Q Rev Biol.* 77(3):261–295.
- Rawles ME. 1963. Tissue interactions in scale and feather development as studies in dermal–epidermal recombinations. *J Embryol Exp Morphol.* 11:765–789.
- Robinson MD, Oshlack A. 2010. A scaling normalization method for differential expression analysis of RNA-seq data. *Genome Biol.* 11(3):R25.
- Robinson MD, Smyth GK. 2008. Small-sample estimation of negative binomial dispersion, with applications to SAGE data. *Biostatistics* 9(2):321–332.
- Rodriguez-Esteban C, Tsukui T, Yonei S, Magallon J, Tamura K, Izpisua Belmonte JC. 1999. The T-box genes *Tbx4* and *Tbx5* regulate limb outgrowth and identity. *Nature* 398(6730):814–818.
- Sawyer RH. 1972. Avian scale development. I. Histogenesis and morphogenesis of the epidermis and dermis during formation of the scale ridge. *J Exp Zool.* 181(3):365–381.
- Sawyer RH, Washington LD, Salvatore BA, Glenn TC, Knapp LW. 2003. Origin of archosaurian integumentary appendages: the bristles of the wild turkey beard express feather-type beta keratins. *J Exp Zool B Mol Dev Evol.* 297(1):27–34.
- Takeuchi JK, Koshiba-Takeuchi K, Matsumoto K, Vogel-Höpker A, Naitoh-Matsuo M, Ogura K, Takahashi N, Yasuda K, Ogura T. 1999. *Tbx5* and *Tbx4* genes determine the wing/leg identity of limb buds. *Nature* 398(6730):810–814.
- Tanaka S, Sugihara-Yamamoto H, Kato Y. 1987. Epigenesis in developing avian scales. III. Stage-specific alterations of the developmental program caused by 5-bromodeoxyuridine. *Dev Biol.* 121(2):467–477.
- Tefft D, Lee M, Smith S, Crowe DL, Bellusci S, Warburton D. 2002. mSprouty2 inhibits FGF10-activated MAP kinase by differentially binding to upstream target proteins. *Am J Physiol Lung Cell Mol Physiol.* 283(4):L700–L706.
- Ting-Berret SA, Chuong CM. 1996. Sonic Hedgehog in feather morphogenesis: induction of mesenchymal condensation and association with cell death. *Dev Dyn.* 207(2):157–170.
- Widelitz RB, Jiang TX, Lu J, Chuong CM. 2000. Beta-catenin in epithelial morphogenesis: conversion of part of avian foot scales into feather buds with a mutated beta-catenin. *Dev Biol.* 219(1):98–114.
- Wu P, Alibardi L, Chuong CM. 2014. Regeneration of reptilian scales after wounding: neogenesis, regional difference, and molecular modules. *Regeneration (Oxf)* 1(1):15–26.
- Wu P, Hou L, Plikus M, Hughes M, Scehnet J, Suksaweang S, Widelitz R, Jiang TX, Chuong CM. 2004. Evo-Devo of amniote integuments and appendages. *Int J Dev Biol.* 48(2–3):249–270.
- Wu P, Jiang TX, Suksaweang S, Widelitz RB, Chuong CM. 2004. Molecular shaping of the beak. *Science* 305(5689):1465–1466.
- Wu P, Ng CS, Yan J, Lai YC, Chen CK, Lai YT, Wu SM, Chen JJ, Luo W, Widelitz RB, et al. 2015. Topographical mapping of  $\alpha$ - and  $\beta$ -keratins on developing chicken skin integuments: functional interaction and evolutionary perspectives. *Proc Natl Acad Sci U S A.* 112(49):E6770–E6779.
- Wu P, Wu X, Jiang TX, Elsey RM, Temple BL, Divers SJ, Glenn TC, Yuan K, Chen MH, Widelitz RB, et al. 2013. Specialized stem cell niche enables

- repetitive renewal of alligator teeth. *Proc Natl Acad Sci U S A*. 110(22):E2009–E2018.
- Xing L, O'Connor JK, McKellar RC, Chiappe LM, Tseng K, Li G, Bai M. 2017. A mid-Cretaceous enantiornithine (Aves) hatchling preserved in Burmese amber with unusual plumage. *Gondwana Res*. 49:264–277.
- Xu X, Zheng X, You H. 2010. Exceptional dinosaur fossils show ontogenetic development of early feathers. *Nature* 464(7293):1338–1341.
- Xu X, Zhou Z, Dudley R, Mackem S, Chuong CM, Erickson GM, Varricchio DJ. 2014. An integrative approach to understanding bird origins. *Science* 346(6215):1253293.
- Zhang Y, Liu T, Meyer CA, Eeckhoutte J, Johnson DS, Bernstein BE, Nusbaum C, Myers RM, Brown M, Li W, et al. 2008. Model-based analysis of ChIP-Seq (MACS). *Genome Biol*. 9(9):R137.
- Zou H, Niswander L. 1996. Requirement for BMP signaling in interdigital apoptosis and scale formation. *Science* 272(5262):738–741.